Development of a Simulation Model of a Self-Energizing Hydraulic Brake to Actively Compensate Brake Torque Oscillations

peer reviewed

Matthias Petry

RWTH Aachen University, Institute for Fluid Power Drives and Controls (IFAS), Aachen, Germany, E-Mail: Matthias.Petry@ifas.rwth-aachen.de

Dr.-Ing. Olivier Reinertz

RWTH Aachen University, Institute for Fluid Power Drives and Controls (IFAS), Aachen, Germany, E-Mail: Olivier.Reinertz@ifas.rwth-aachen.de

Professor Dr.-Ing. Hubertus Murrenhoff

RWTH Aachen University, Institute for Fluid Power Drives and Controls (IFAS), Aachen, Germany, E-Mail: post@ifas.rwth-aachen.de

Abstract

Friction force oscillations caused by changing properties of the contact zone between brake disc and pad are well known from various applications. Resulting effects like brake judder are known phenomena in brake technologies and in the scope of various scientific work. A new measure to potentially reduce brake torque oscillations is the active compensation with the use of the control system of a self-energizing hydraulic brake (SEHB). New in comparison to traditional disc brakes is the fact that the brake torque is measured by the pressure in an additional supporting cylinder. Thus, the brake system is able to work in brake torque control mode. Within this paper a dynamic simulation model of the SEHB is shown and evaluated with measurement data achieved from a full scale test rig for railway applications. Based on the simulation model a pressure control strategy is developed to minimize brake torque oscillations of lower frequencies. The control parameters of the simulation are transferred to the experimental setup. Finally, simulation and experimental results are compared. Future work will deal with the development of control strategies to additionally minimize brake torque oscillations of the higher dynamics.

KEYWORDS: SEHB, Simulation, Brake Torque Oscillations, Control Strategies

1. Introduction

Oscillations of the braking torque are caused both by dynamic changes of the friction coefficient between brake pads and disc and by deviations of the contact pressure. Main excitation mechanisms are reversible deformation of the brake disc and permanent disc thickness variations. In practice, relevant effects are brake squealing and judder /1/. Especially sideface runout (SRO) and waviness of the disc are relevant problems and can lead to reduced comfort, increased noise and damage /2/. A commonly used countermeasure consists of applying smallest tolerances during production and mounting process of the disc and fine-tuning of the brake clearance, which can lead to higher costs and increased development time. An alternative approach is the use of the dynamic properties of the control system of a self-energizing hydraulic brake (SEHB). The author´s research group at the Institute for Fluid Power Drives and Controls (IFAS) of RWTH Aachen University developed a brake system for railway applications which is able to generate the needed power from the brake process itself /3/. The system profits from the high power density of hydraulic actuation /4/ and the good dynamics of the control system /5/. In this paper the influence of the existing brake disc waviness of the SEHB and the development of a simulation model of the brake system is shown. Further, a control strategy with predicative intrusion for compensating brake torque oscillations will be introduced.

2. SEHB

2.1. Operating Principle

The brake system layout of the investigated SEHB is shown in **Figure 2.1**. The brake system is tailored to railway applications and mainly consists of the brake pads, brake calipers, a brake actuator and a control valve. The brake actuator clamps the brake hydraulically. In contrast to conventional disc brakes, the SEHB utilises an additional supporting cylinder. To explain the operation principle consider a regular braking process: to begin braking, the control valve is opened from neutral position. Pressurized oil stored in a high-pressure accumulator flows towards the piston end of the brake actuator. The stroke of the brake actuator causes the brake pads to be pressed onto the brake disc. Hence, a normal force is applied and a friction force develops. This force causes the caliper to move in the tangential direction. Due to this movement the brake caliper exerts a force on the supporting cylinder. In doing so, pressure builds up in the chamber of the supporting cylinder. As the control valve is still open, the pressurized oil is continuously fed to the piston end of the brake actuator, increasing the clamping force. In this way the self-energization loop is closed.

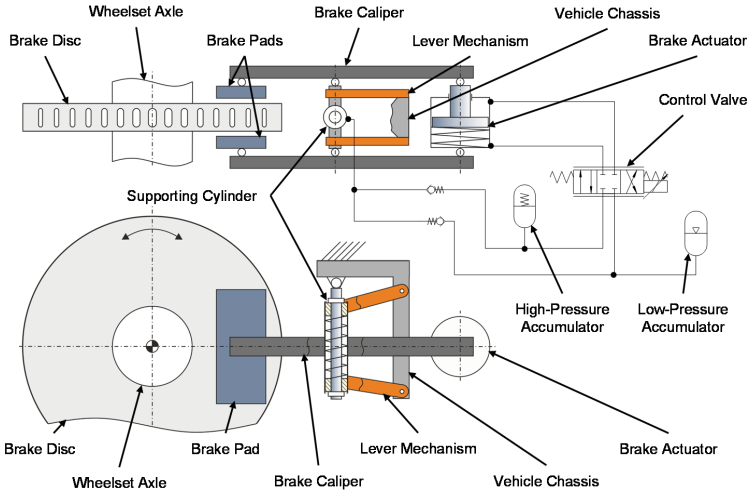

Figure 2.1: Principle of the SEHB

2.2. Test Rig

Experiments are conducted using a full scale test rig for railway brake applications in the IFAS laboratory. In contrast to conventional brake tests which use electric motors to drive the brake shaft the test rig for this study uses a hydraulic drive, which operates in a secondary control loop with the rotational speed *n* as the control variable /6/. Due to the high power density higher rotational speeds can be held constant over a large range of generated braking torques. Further, specific deceleration rates similar to the real loads of the railway vehicle can be achieved.

2.3. Force Oscillation by Brake Disc Waviness

The test rig is equipped with an internally ventilated brake disc (d_{BD} = 640 mm) which has run several brake cycles, so that the topography of the surface is measured and the disc is checked for visible cracks before the experiments are conducted. **Figure 2.2** provides the disc thickness variation (DTV) for both sides along the middle friction radius. High brake loads have obviously lead to permanent deformation of the brake disc surface. A dominant waviness of 2nd order can be seen clearly for both sides with an antisymmetric distribution. The used brake pad halves correspond to International Union of railways (UIC) standards and are made from organic material. During a brake process pressure oscillations can be observed in both hydraulic cylinders (Figure 2.2 bottom). Strong time dependent behaviour from the rotational speed allows the conclusion of brake disc waviness of 2nd order as the dominant excitation, which corresponds to the literature /2/.

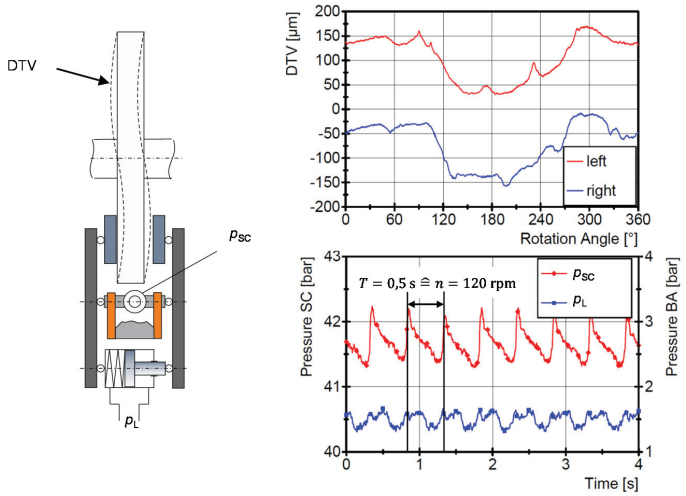

Figure 2.2: Brake disc DTV and pressure oscillations

3. Simulation Model

To develop and test control strategies for compensation of brake torque oscillations a simulation model of the SEHB is implemented into the one-dimensional simulation tool DSHplus. First the actuation force which reacts in normal direction between brake pads and brake disc is implemented. Second the brake force and pressure into the supporting cylinder are calculated with respect to the frictional coefficient and the brake disc waviness. The pressure feedback from the supporting cylinder to the valve (Figure 2.1) which closes the circuit of self-energization is not considered in this stage of simulation.

3.1. Actuation Force

Figure 3.1 shows the hydraulic-mechanical actuation system of the SEHB. The hydraulic part consists of the control valve, hydraulic lining, and the brake actuator. The direct driven control valve is designed for a 4/3-way operation with zero-overlap and small nominal volume flow. It operates in position control mode and shows a eigenfrequency f_V = 225 Hz and damping factor D_V = 0,6. The eigenfrequency f_{BA} of the brake actuator can be determined by (1) /4/.

$$f_{\mathrm{BA}} = \frac{1}{2\pi}\sqrt{\frac{c_{\mathrm{Fl,A}} + c_{\mathrm{Fl,B}} + c_{\mathrm{Sp,BA}}}{m_{\mathrm{BA,2}}}} = 1181\ \mathrm{Hz} \tag{1}$$

The influence of the mechanical part of the actuation system is difficult to analyse due to its complexity. Figure 3.1 illustrates its reduction to a spring and mass system. The most important parts are the calipers, bearings, pad holder (PH), and brake pads (BP).

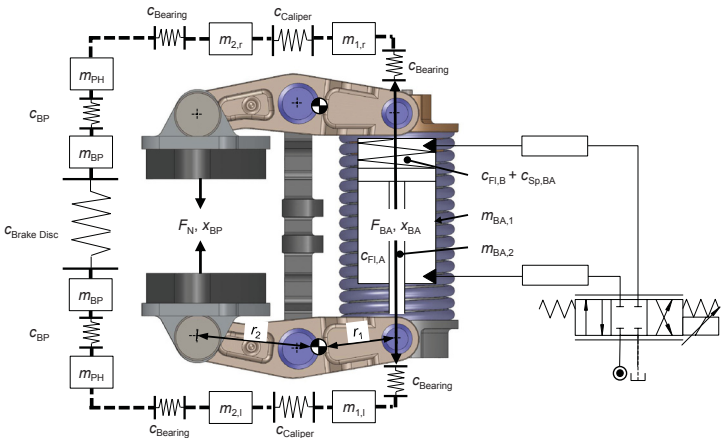

Figure 3.1: Hydraulic-mechanical structure of the actuation system (top view)

Caliper and bearing stiffness are determined experimentally by measuring relative positions of involved components under various loads. The reduced masses $m_{1,r/l}$ and $m_{2,r/l}$ which interact via the caliper stiffness can be determined with both the condition of conservation of mass (2) and position of centre of mass (3) /7/.

$$m_{\mathrm{Cal}} = m_1 + m_2 \tag{2}$$

$$r_1 m_1 = r_2 m_2 \tag{3}$$

Hence, the reduced masses are calculated by (4) and (5).

$$m_1 = m_{\mathrm{Cal}} \frac{r_2}{r_1 + r_2} \tag{4}$$

$$m_2 = m_{\mathrm{Cal}} \frac{r_1}{r_1 + r_2} \tag{5}$$

The stiffness of the brake pads is calculated by (6) regarding the nominal friction area A_{BP}, the nominal bulk modulus E_{BPn}, and the thickness b_{BP} of the pads.

$$c_{\mathrm{BP}} = \frac{E_{\mathrm{BP}} A_{\mathrm{BP}}}{b_{\mathrm{BP}}} \tag{6}$$

Figure 3.2 left presents the amplitude response of the mechanical part of the actuation system. The main peak can be observed at a frequency of 570 Hz. A smaller peak occurs at 200 Hz. Consider that damping factors are set very low in the simulation because experimental data were not available. Subsequently, excitation frequencies due to the rotational speed and DTV reach 25 Hz at 1500 rpm. Results from simulation and measurement of an actuation process are illustrated in figure 3.2 right and show good agreement. The measured force is determined by a load sensor between the

brake pads instead of the brake disc. The stiffness of the brake disc was replaced considering the stiffness of the load sensor. During start up high forces are caused by the spring force of the brake actuator, which leads to a minimal demanded normal force in case of hydraulic failure.

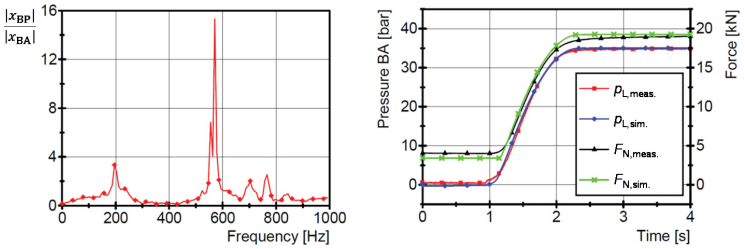

Figure 3.2: Amplitude response of the mechanical part of the actuation system (left), simulated and measured actuation process (right)

3.2. Brake Force and Supporting Cylinder Pressure

During the brake process an additional force F_{BD} caused by the brake disc waviness occurs next to the force F_N by the actuation system and effects the total force $F_{N,tot}$ between brake pad and disc (7). F_{BD} can be calculated by the measured DTV and the brake disc stiffness and leads to a deviation of the supporting cylinder force F_{SC} (8) depending on the rotation angle of the brake disc.

$$F_{\mathrm{N,tot,l/r}} = F_{\mathrm{N,l/r}} + F_{\mathrm{BD,l/r}} = F_{\mathrm{N,l/r}} + c_{\mathrm{BD}} x_{\mathrm{BD,l/r}} \tag{7}$$

$$F_{\mathrm{SC}} = \mu i_{\mathrm{SC}} \left(F_{\mathrm{N,tot,l}} + F_{\mathrm{N,tot,r}} \right) \tag{8}$$

Figure 3.3 left depicts the map-based implementation of the DTV and the determination of the brake and supporting cylinder force. Due to the high stiffness of the mechanical structure compared with the stiffness of the oil volume in the supporting cylinder, the detailed implementation of a further spring and mass system is neglected. The supporting cylinder pressure is calculated by (9), where $F_{SP,SC}$ considers the force of the spring which retracts the brake to its initial position after the brake process and $F_{fr,SC}$ the friction forces.

$$p_{\mathrm{SC}} = \frac{F_{\mathrm{SC}} - F_{\mathrm{Sp,SC}} - F_{\mathrm{fr,SC}}}{A_{\mathrm{SC}}} \tag{9}$$

When measuring the supporting cylinder pressure over increasing actuation force an increase of the friction coefficient can be observed which leads to higher pressure oscillations (Figure 3.3, top right). This behaviour is typical for brake pads made from organic materials and depends on the area of real contact, load, and time /8/.

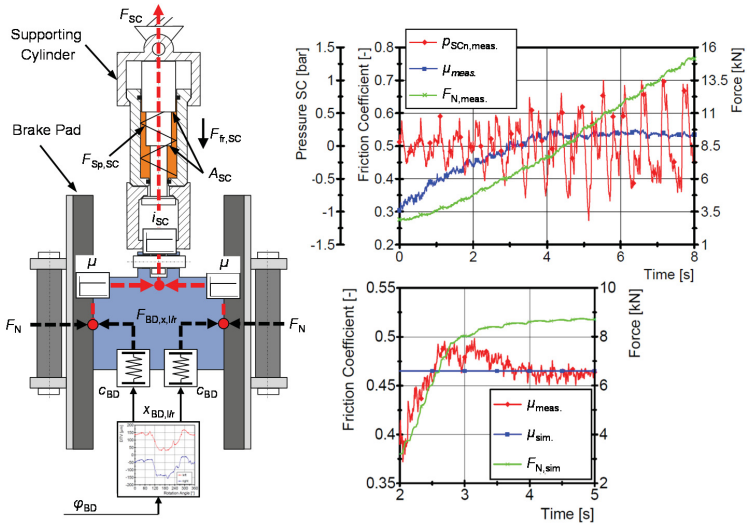

Figure 3.3: Brake force / DTV implementation (left); pressure oscillations at rising friction coefficient (right top); declining behaviour at load jump (right bottom)

When increasing the load the area of real contact between brake pad and disc will be smaller than the steady-state size until it reaches its maximum. Further, a reduction in the friction coefficient can be observed after a fast rise of the force and reaching a constant load (Figure 3.3, right bottom). Here, slower processes like cleaning contact plateaus from binder material during the brake process lead to a diminished area of real contact and thus to a lower friction coefficient. A detailed model of the friction coefficient which includes the dependence of the area of real contact, participating elements of the material compound, exact thermo-mechanical loads, and time-depending behaviour is outside the scope of this work. To obtain a simulation tool for developing control strategies for brake force oscillations of small amplitude compared to absolute values the friction coefficient is set to a constant value. Deviations of experimental results are corrected afterwards with the constantly measured friction coefficient to check the simulation results.

Figure 3.4 left depicts the simulated and measured pressure increase at maximum brake force and back. Pressure levels and gradients show good agreement between simulation and experiment. Only at the end of ramps the simulation results are higher due to the reduction in the friction coefficient. Pressure oscillations of the supporting cylinder, reduced by the mean value, at a constant friction coefficient $\mu \approx 0{,}43$ are illustrated in Figure 3.4 right.

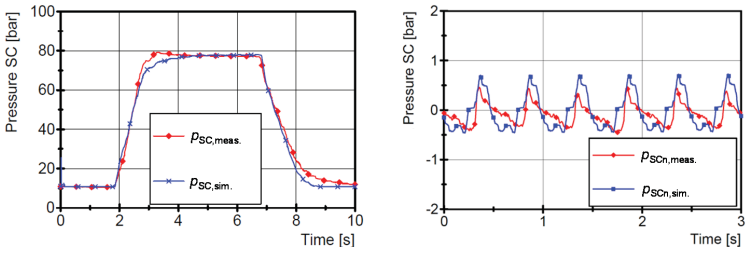

Figure 3.4: Jump of the supporting cylinder pressure (left); pressure oscillations (right)

4. Control Strategies to Compensate Brake Torque Oscillations

The simulation model is enlarged to a closed loop control system to develop a controller design to compensate the brake torque oscillations. Subsequently, the obtained control parameters are transferred to the test rig.

4.1. Brake Torque Control with P-Controller

A simple method to implement a brake torque control with the SEHB is the use of a controller with proportional behaviour. **Figure 4.1** left illustrates the principle. The desired brake torque is compared with the current value calculated from the measured supporting cylinder pressure. When the control deviation is multiplied by the factor K_P and the output sent to the control valve, the control loop is closed. As described the disturbance variable of the brake disc waviness influences p_{SC} immediately. Varying K_P over a broad range leads to only small changes of pressure oscillations in simulation (Figure 4.1 right). When K_P is further increased instability occurs. Data from measurements confirm the simulation results while instability is already reached at K_P = 0,01.

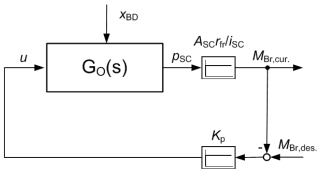

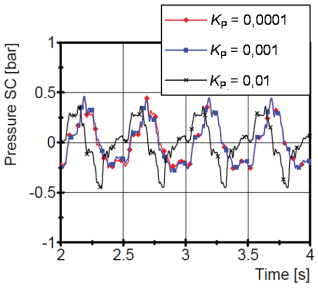

Figure 4.1: Proportional brake torque control (left); simulation results with varying K_P

4.2. Brake Torque Control with Predicative Disturbance Decoupling

Due to the limited effect of only instantaneous control strategy with proportional behavior a predicative disturbance decoupling on the control signal is developed

(**Figure 4.2**). The control signal u is calculated from the signal u_P of the P-controller which is set to a value which shows good dynamics and stability of the system and an additional signal u_{PSB}. The predicative signal builder (PSB) makes use of the time-depending behaviour of the pressure oscillations generating a sinusoidal signal anticyclical to the brake torque oscillations. This leads to increasing actuation force during brake force decrease.

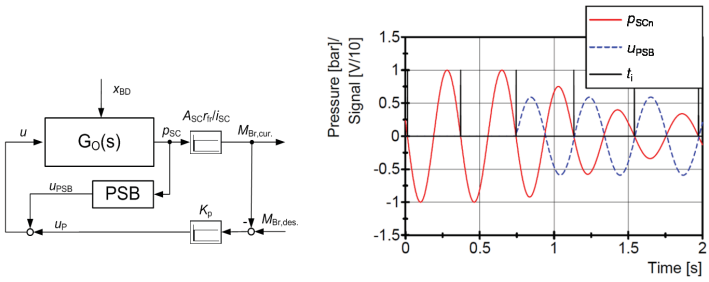

Figure 4.2: Brake torque control including predicative intrusion signal

The additional signal $u_{PSB,i+1}$ is found by (10) under assumption of a constant deceleration of the brake.

$$u_{\mathrm{PSB,i+1}} = \hat{A}\sin\left(2\pi\left(t_i + 1{,}5(t_\mathrm{i} - t_{\mathrm{i}-1})\right) + \varphi\right) \tag{10}$$

By measuring the time between every revolution of the pressure the time difference can be determined and the revolution time of the next pressure oscillation can be foreseen. The gain factor is fixed by the amplitude $\hat{A}$ while the phase shift φ considers the delay time between valve stroke and increase of the load pressure. **Figure 4.3** illustrates simulated and measured results of pressure oscillations at brake torque M_{Br} = 1 kNm, constant rotational speed n = 120 rpm and a friction coefficient $\mu \approx 0{,}5$.

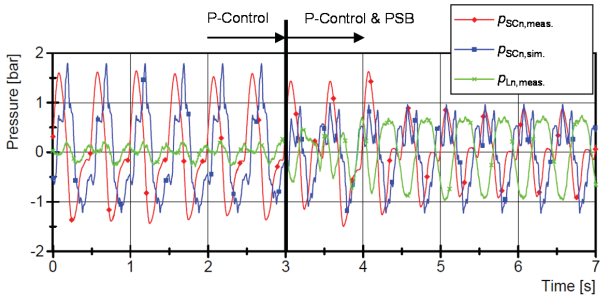

Figure 4.3: Pressure oscillations with predicative disturbance decoupling

When enabling the predicative signal u_{PSB}, the load pressure deviation p_{Ln} changes from cyclical to anticyclical oscillation with increasing amplitude compared to the

supporting cylinder pressure p_{SCn}. Thus, the amplitudes of the supporting cylinder pressure are reduced by about 40% after a short settling time. A further reduction could be reached by increasing the fixed amplitude $\hat{A}$ of u_{PSB}, but must be considered, that a minimum oscillation of the supporting cylinder pressure has to be obtained to detect the impact of the brake disc waviness. **Figure 4.4** shows the amplitude reduction of the supporting cylinder pressure during a brake process with constant deceleration.

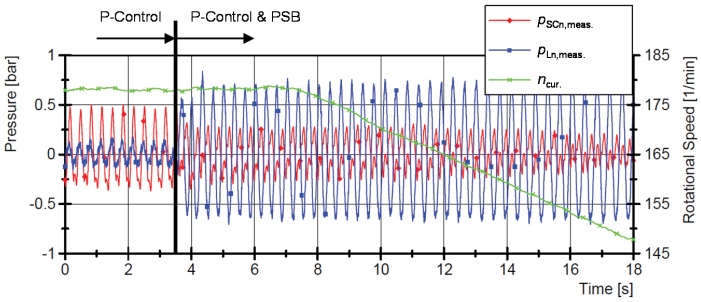

Figure 4.4: Effect of predicative disturbance decoupling at decreasing rotational speed

Again, pressure amplitudes are reduced by enabling the additional disturbance decoupling. When decreasing the rotational speed, the anticyclical oscillation of the load pressure fits the pressure oscillations of the supporting cylinder. A further amplitude reduction at lower speed can be observed and indicates that the fixed amplitude $\hat{A}$ of the predicative intrusion signal u_{PSB} could be optimized depending on the point of operation.

5. Conclusion and Outlook

In accordance to commonly used brake discs, the brake disc in the IFAS test rig shows a permanent thickness variation of 2nd order which leads to an excitement of the brake torque during the brake process. By developing a simulation model of the SEHB in the software DSHplus an effective tool was created to develop and test control strategies for compensating observed brake torque oscillations. The implementation of the actuation system shows good agreement between simulation and experimental results. Furthermore, a critical influence of the exciting mechanism of the brake disc waviness could be excluded by investigating the dynamic properties of the complex hydraulic-mechanical actuation structure. When implementing the brake force and the pressure in the supporting cylinder the influence of the brake disc waviness was considered. A dependence of the friction coefficient on brake load and time was observed. However, measured influences were neglected due to steady-state operating points and a lack of an appropriate model. After validating the simulation model with experimental results a

simple proportional control was tested which shows no recognizable compensation of the brake torque oscillations. By using an additional predicative disturbance decoupling the actuation force could be modified to achieve a reduction of 40 to 50% depending on gain and rotational speed. Future work will be the extension of the additional predicative signal builder by adapting the gain factor to varying operating points. The influence of closing the circuit of self-energization will be investigated by simulation and experiments. Finally, the achieved control system will be tested at operating points with higher frequency excitations and resulting brake torque oscillations.

6. Acknowledgments

This work was funded by the German Research Foundation (DFG) in the scope of the project “Selbstverstärkende Elektro-Hydraulische Bremse” (MU 1225/34-3). The authors would like to thank DFG for its support.

7. References

/1/ Wallaschek J., Hach K.H., Stolz U., and Mody P., 1999, “A survey of the present state of friction modelling in the analytical and numerical investigation of brake noise generation”, in Proc. of the ASME Vibration Conference, Las Vegas, USA

/2/ Bittner C., 2006, “Reduzierung des Bremsenrubbelns bei Kraftfahrzeugen durch Optimierung der Fahrwerksauslegung”, Ph.D thesis, TU München, Germany

/3/ Ewald J., 2011, “Selbstverstärkende Elekto-Hydraulische Bremse (SEHB) für Schienenfahrzeuge”, Ph.D. thesis, RWTH Aachen University, Germany

/4/ Murrenhoff, H., 2008, “Servohydraulik – Geregelte hydraulische Antriebe”, 3rd ed., Shaker, Aachen, Germany

/5/ Kühnlein M., 2013, “Selbstverstärkende Elektro-Hydraulische Bremse mit hoher Systemdynamik”, Ph.D. thesis, RWTH Aachen University, Germany

/6/ Lamjahdy A., Moussa N., Hirtz M., Dufrenoy P., Weichert D., Murrenhoff H., Markert B., 2015, “Simulation of thermal gradients on hot bands of disc brakes“, in Proc. of FISITA Eurobrake Conference, Dresden, Germany

/7/ Corves B., 2011, “Grundlagen der Maschinen- und Strukturdynamik“, lecture notes, RWTH Aachen University, Germany

/8/ Eriksson M, Bergman F., Jacobson S., 2002, “On the nature of tribological contact in automotive brakes”, Wear Vol. 252, pp. 26-36

8. Nomenclature

A	Area	mm²
$\hat{A}$	Signal amplitude	V
b_{BP}	Thickness of brake pad	mm
c, c_{Fl}	Spring constant, stiffness of fluid	N/m
D	Damping	-
E	Bulk modulus	N/m²
i_{SC}	Transmission ratio to supporting cylinder	-
f	Frequency	Hz
F	Force	N
m	Mass	kg
M_{Br}	Brake torque	Nm
n	Rotational speed	rpm
p	Pressure	bar
r	Lever arm	mm
t, T	Time	s
u	Control signal	V
x	Position	mm
α	Area ratio	-
φ	Phase shift, rotation angle	rad
μ	Friction coefficient	-